Abnormal lymphangiogenesis in idiopathic pulmonary fibrosis with insights into cellular and molecular mechanisms

Souheil El-Chemaly[a], Daniela Malide[b], Enrique Zudaire[c], Yoshihiko Ikeda[a,1], Benjamin A. Weinberg[b], Gustavo Pacheco-Rodriguez[a], Ivan O. Rosas[a,2], Marta Aparicio[c], Ping Ren[a], Sandra D. MacDonald[a], Hai-Ping Wu[a], Steven D. Nathan[d], Frank Cuttitta[c], J. Philip McCoy[e], Bernadette R. Gochuico[f], and Joel Moss[a,3]

[a]Translational Medicine Branch, [b]Light Microscopy Core Facility, and [e]Flow Cytometry Core Facility, National Heart, Lung, and Blood Institute, National Institutes of Health, Bethesda, MD 20892; [c]Angiogenesis Core Facility, National Cancer Institute, National Institutes of Health, Gaithersburg, MD 20877; [d]Advanced Lung Disease and Transplant Program, Inova Heart & Vascular Institute, Inova Fairfax Hospital, Falls Church, VA 22042; and [f]Medical Genetics Branch, National Human Genome Research Institute, National Institutes of Health, Bethesda, MD 20892

Communicated by Martha Vaughan, National Heart, Lung, and Blood Institute, Bethesda, MD, December 31, 2008 (received for review December 1, 2008)

Idiopathic pulmonary fibrosis (IPF) is a chronic, progressive, debilitating respiratory disease whose pathogenesis is poorly understood. In IPF, the lung parenchyma undergoes extensive remodeling. We hypothesized that lymphangiogenesis is part of lung remodeling and sought to characterize pathways leading to lymphangiogenesis in IPF. We found that the diameter of lymphatic vessels in alveolar spaces in IPF lung tissue correlated with disease severity, suggesting that the alveolar microenvironment plays a role in the lymphangiogenic process. In bronchoalveolar lavage fluid (BALF) from subjects with IPF, we found short-fragment hyaluronic acid, which induced migration and proliferation of lymphatic endothelial cells (LECs), processes required for lymphatic vessel formation. To determine the origin of LECs in IPF, we isolated macrophages from the alveolar spaces; CD11b$^+$ macrophages from subjects with IPF, but not those from healthy volunteers, formed lymphatic-like vessels in vitro. Our findings demonstrate that in the alveolar microenvironment of IPF, soluble factors such as short-fragment hyaluronic acid and cells such as CD11b$^+$ macrophages contribute to lymphangiogenesis. These results improve our understanding of lymphangiogenesis and tissue remodeling in IPF and perhaps other fibrotic diseases as well.

endothelial cell | hyaluronan | idiopathic pulmonary fibrosis | lymphangiogenesis | macrophage

Idiopathic pulmonary fibrosis (IPF) is a chronic, progressive, and often fatal lung disease of unknown etiology, characterized by the insidious onset of interstitial infiltrates in the lung parenchyma associated with progressive dyspnea due to ventilatory restriction (1). The pathogenesis of usual interstitial pneumonia (UIP), the pathological correlate of IPF, is poorly understood. An inflammatory response has been described as an early step in the progression of UIP, leading to the development of lymphoid structures, a hallmark of chronic inflammation (2). Currently, a prevailing hypothesis is that IPF is caused by dysregulation of epithelial and mesenchymal cells. In this model, activation of epithelial cells leads to the release of fibrogenic molecules and cytokines, which stimulates the differentiation of mesenchymal cells and promotes lung fibrosis (3).

There is a paucity of data regarding tissue fibrosis and lymphangiogenesis. The fibrotic process in a rat remnant kidney model was associated with newly formed lymphatic vessels (4). In bleomycin-induced lung injury, data suggest that the angiogenic process is followed by lymphangiogenesis (5).

Inflammatory molecules and cells are recognized as important contributors to lymphangiogenesis in animal models (6) and in human disease (7–9). Cytokines (e.g., IL-1β, TNF-α) induce the expression of VEGF-C and other growth factors that are key mediators of lymphangiogenesis (10). Moreover, hyaluronic acid, a critical factor in lung injury and repair, is known to induce lymphangiogenesis (11). LYVE-1, a CD44 homolog and receptor for hylauronic acid, is a known surface protein of lymphatic endothelial cells (LECs) (12). Although lymphatic vessels can arise from vacuolization of LECs that merge to form lymphatic tubes (13), activated CD11b$^+$ macrophages also can form lymphatic tubes by a putative transdifferentiation process (6). Given that alveolar macrophages represent a major constituent of bronchoalveolar cells and that elevated concentrations of lung cytokines, chemokines, and hyaluronic acid is a feature of IPF, we hypothesized that lymphangiogenesis could occur in IPF.

To study lymphangiogenesis in IPF, we identified lymphatic vessels in IPF lung tissue and investigated possible cellular and molecular mechanisms that could contribute to the lymphangiogenic process. We found that the lymphatic vessels in the IPF lung increase in diameter with increasing disease severity. We also determined that hyaluronan fragments and CD11b$^+$ macrophages found in the IPF lung contribute to the lymphangiogenic process. Together, these findings suggest that lymphatic vessel development may contribute to the pathogenesis of IPF and could serve as a rational drug target for future IPF therapy.

Results

Alveolar Lymphangiogenesis Is a Feature of IPF. To define lymphatic vessels in normal and IPF lung, tissue sections were immunostained with anti-podoplanin antibodies. In normal lung tissue, lymphatic vessels reactive with anti-podoplanin antibodies are found proximal to large anti-CD34–reactive blood vessels. In normal alveolar spaces, small CD34-positive capillaries were found, but no immunoreactivity for podoplanin was detected (Fig. 1*A*). In marked contrast, positive immunoreactivity for podoplanin was found in alveoli of subjects with IPF of varying severity, indicating the presence of LECs lining large and small lymphatic vessels (Fig. 1*B–D*, arrows). In the IPF lung, unlike in normal tissue, lymphatic distribution was not limited to the proximity of large blood vessels; lymphatic structures were

Author contributions: S.E.-C., D.M., E.Z., G.P.-R., B.R.G., and J.M. designed research; S.E.-C., D.M., E.Z., Y.I., M.A., S.D.M., F.C., J.P.M., and B.R.G. performed research; I.O.R., S.D.N., F.C., and B.R.G. contributed new reagents/analytic tools; S.E.-C., D.M., E.Z., B.A.W., G.P.-R., P.R., H.-P.W., J.P.M., and J.M. analyzed data; and S.E.-C., D.M., G.P.-R., B.R.G., and J.M. wrote the paper.

The authors declare no conflict of interest.

Freely available online through the PNAS open access option.

[1]Present address: Department of Pathology, National Cardiovascular Center 5–7-1, Fujishirodai, Suita, Osaka 565-8565, Japan.

[2]Present address: Department of Medicine, Division of Pulmonary and Critical Care Medicine, Brigham and Women's Hospital, Harvard Medical School, Boston, MA 02115.

[3]To whom correspondence should be addressed. E-mail: mossj@nhlbi.nih.gov.

This article contains supporting information online at www.pnas.org/cgi/content/full/0813368106/DCSupplemental.

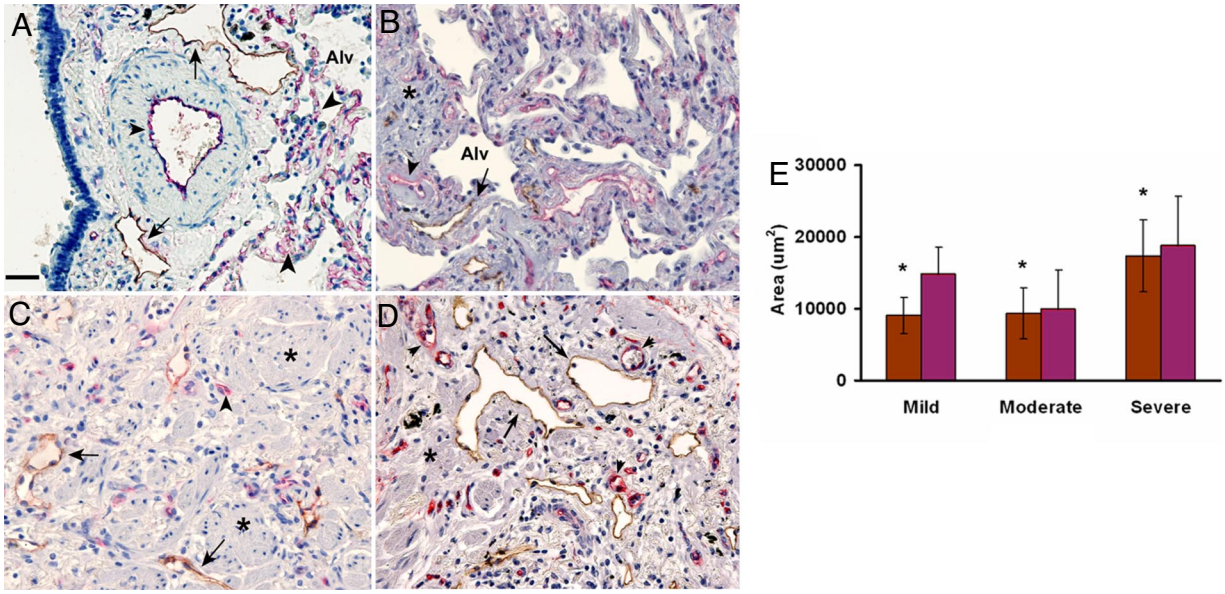

Fig. 1. Lymphatic vessel area increases in parallel with disease severity in IPF tissue sections. (*A*) In normal human lung, large lymphatic vessels (in brown, arrows) appear only along large blood vessels (in red, arrowheads), whereas only CD34-positive endothelial cells without lymphatics line the distal alveolar spaces (Alv). (*B–D*) In tissue sections from subjects with mild (*B*), moderate (*C*), and severe (*D*) IPF, there is an marked increase of both lymphatic and blood capillary vessels adjacent to the alveolar spaces earlier in disease (*B*), with further increase in areas of fibrosis (*). (Magnification bar: 50 μm.) (*E*) Tissue sections were stained with D2–40 (brown) and CD-34 (red) antibodies. Images (n = 15) of each section were obtained. ImageJ image analysis software was used to measure the area of lymphatic vessels (D2–40–positive) and blood vessels (CD34-positive) in tissue sections from mild (n = 3), moderate (n = 5), and severe (n = 4) IPF. A statistically significant increase in average lymphatic area with increasing disease severity is seen ($P < .05$, severe compared with mild and moderate).

contiguous to relatively normal alveolar spaces (Fig. 1*B*) and throughout the fibrotic tissue (Fig. 1*C* and *D*). In addition, CD34 immunostaining in IPF was detected in normal and fibrotic alveoli. At their periphery, fibroblastic foci, histological hallmarks of IPF, were reactive with both anti-podoplanin and anti-CD34 antibodies [supporting information (SI) Fig. S1]. Negative controls with nonimmune IgG exhibited no immunoreactivity (Fig. S2*A*). Positive controls with both anti–D2–40 and anti–CD34 antibodies using placental tissue are shown in Fig. S2 *B* and *C*.

Lymphatic Area Correlates with Disease Severity in IPF. The number, area, and perimeter of lymphatic and blood vessels were quantified using immunostained lung tissue from subjects with IPF. Our data demonstrated that the mean area and perimeter, but not number, of lymphatic vessels correlated with disease severity (P = .009, .005, and .18, respectively) (Fig. 1 and Table S1). In contrast, the number, but not area or perimeter, of blood capillaries correlated with disease severity (P = .003, .18, and .17, respectively). Analysis of the total area of lymphatic and blood vessels per tissue section showed that mean area of lymphatic vessels, but of not blood capillaries, increased significantly with disease severity (P = .024 and .117, respectively) (Table S1).

LYVE-1 and Hyaluronic Acid in IPF and Normal Lung. LECs are characterized by the presence of LYVE-1, a CD44 homolog and receptor for hyaluronic acid, a chemoattractant for endothelial cells found in high concentrations in inflammation and lung injury (12). Immunostaining for LYVE-1 in normal lung tissue sections showed a distribution similar to that of podoplanin in contiguity of large blood vessels and airways (Fig. S3). In contrast, IPF lung revealed vessels positive for LYVE-1 and podoplanin across tissue sections (Fig. 2*A* and *B* and Fig. S4). In normal lung, signal from hyaluronic acid binding protein was weak and localized to alveolar walls (Fig. S5); in IPF lung, hyaluronic acid staining localized in areas of fibroblastic proliferation and alveolar walls (Fig. 2*D* and *F* and Fig. S5). The specificity of the reaction was confirmed by the absence of staining in samples pretreated with hyaluronidase before immunoreaction (Fig. 2*H*).

Prolymphangiogenic Proteins in BALF. To investigate for soluble prolymphangiogenic factors in the lung, BALF samples from 15 subjects with IPF and 14 healthy volunteers were analyzed. As shown in Table 1, concentrations of monocyte chemotactic protein (MCP)-1, hepatocyte growth factor (HGF), and tissue inhibitor of metalloproteinase (TIMP)-1 were markedly higher in the BALF samples from subjects with IPF (13.8 ± 2.5, 13.2 ± 2.9, and 202 ± 30.1 ng/mL, respectively) compared with those from healthy volunteers (6.2 ± 3, 7.4 ± 1.1, and 141 ± 31 ng/mL, respectively) ($P < .05$). Conversely, concentrations of VEGF and VEGF-C were significantly higher in the BALF samples from healthy volunteers (43.1 ± 10.5 and 9.2 ± 1.5 ng/mL, respectively) compared with those from the subjects with IPF (4.6 ± 0.9 and 2.6 ± 0.6 ng/mL, respectively) ($P < .0001$). VEGF-D concentrations did not differ significantly between the 2 groups (9.9 ± 5.5 vs. 6.1 ± 2.7 ng/mL; $P > .05$). Concentrations of CCL21, a chemokine secreted by LECs, were significantly higher in the subjects with IPF (1.22 ± 0.23 vs. 0.76 ± 0.09 pg/mL; P = .029).

BALF from Subjects with IPF Induces Increased LEC Migration, an Effect Enhanced by Treatment with Hyaluronidase. To assess the potential effects of soluble factors in BALF on lymphangiogenesis, samples from healthy volunteers and subjects with IPF were added to endothelial cells in migration assays. The samples from healthy volunteers caused no statistically significant increase in LEC migration ($P > .05$), but the samples from the subjects with IPF produced a significant increase in LEC migration ($P < .005$) (Fig. 3). Migration assays using BALF samples that had been incubated with function-blocking antibodies against MCP-1, HGF, and TIMP-1 (factors elevated in BALF from the subjects with IPF) demonstrated no statistically significant change in LEC migration pattern (data not shown).

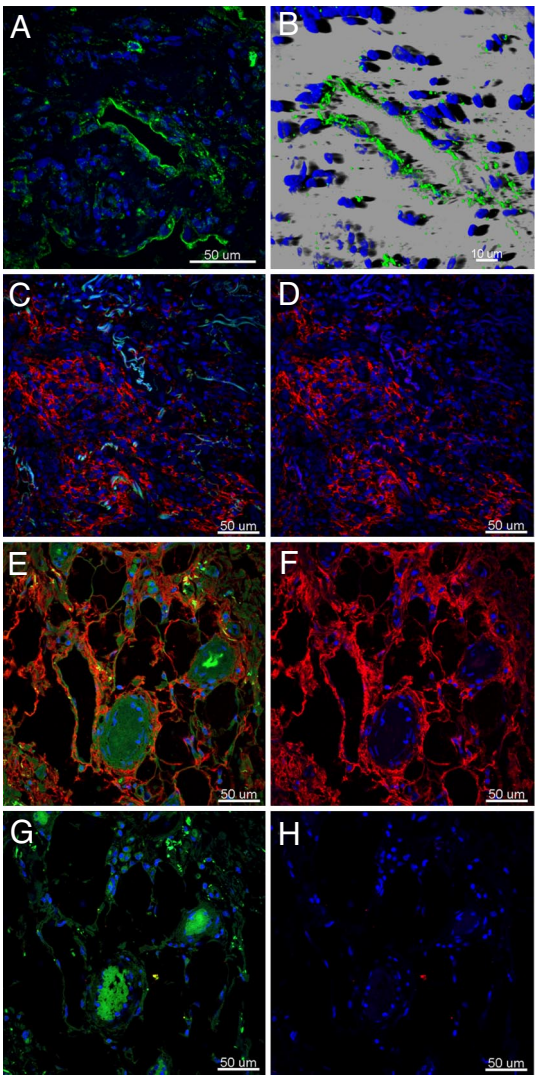

Fig. 2. Presence of hyaluronic acid and LYVE-1–positive vessels in IPF lung. Immunofluorescence staining of paraffin-embedded sections of IPF lung tissue shows LYVE-1 (green) in lymphatic vessels in a representative single confocal microscopy optical section (*A*) and in 3-dimensional reconstruction images of lymphatic vessels (*B*). Fibroblastic areas (*C* and *D*) and alveolar walls (*E* and *F*) displaying positive staining for hyaluronic acid (red) are presented as merged images of hyaluronic acid (red), DAPI (blue) with (*C* and *E*) or without (*D* and *F*) an autofluorescence signal (green). Pretreatment of the tissue sections with hyaluronidase abolished hyaluronic acid reactivity (*G* and *H*), whereas autofluorescence remained unchanged (*G*). Cell nuclei were stained with DAPI (blue).

When cleaved by hyaluronidase, hyaluronic acid (or hyaluronan), a ligand that binds to many cell surface receptors present on the surface of LECs, generates small-fragment hyaluronic acid (14), which has increased activity (15). Agarose gel electrophoresis found that BALF from subjects with IPF at baseline contained both large- and short-fragment hyaluronic acid. After hyaluronidase treatment, almost all of the large-fragment hyaluronic acid was eliminated, and the amount of short-fragment hyaluronic acid subsequently increased (data not shown). To explore the role of short-fragment hyaluronic acid in migration and proliferation, IPF BALF with and without hyaluronidase treatment was used in migration and proliferation experiments. Hyaluronidase-treated IPF BALF caused a statistically significant increase in LEC migration and proliferation compared with untreated IPF BALF ($P < .05$ and .01, respectively) (Fig. 3*B* and *C*). Moreover, the addition of short-fragment hyaluronic acid to healthy volunteer BALF resulted in a statistically significant increase in LEC migration (Fig. S6).

Table 1. Concentrations of lymphangiogenic proteins in BALF samples from subjects with IPF and healthy volunteers

	IPF subjects (n = 15)	Healthy volunteers (n = 14)	*P* value
VEGF-D, ng/mL	9.9 ± 5.5	6.1 ± 2.747	.239
VEGF-C, ng/mL	2.6 ± 0.67	9.3 ± 1.6	<.005
VEGF, ng/mL	4.6 ± 9.4	43.1 ± 10.6	<.005
FGF, ng/mL	0.67 ± 0.11	0.89 ± 0.21	.366
HGF, ng/mL	13.2 ± 2.9	7.4 ± 1.2	.031
MCP-1, ng/mL	13.8 ± 2.5	6.2 ± 3.0	.026
TIMP-1, ng/mL	202 ± 30.1	140.8 ± 30.7	.019
TIMP-2, ng/mL	66.1 ± 11.7	65.9 ± 9.7	.903
CCL21, pg/mL*	1.220 ± 0.232	0.766 ± 0.091	.029

Values are reported as mean ± SD.
*Quantification of CCL21 was performed separately in BALF samples from 30 subjects with IPF and 65 healthy volunteers.

CD11b$^+$ Macrophages from Subjects with IPF Form Lymphatic-Like Tubes in Vitro. It has been suggested that CD11b$^+$ macrophages are capable of forming lymphatic tubes both in vivo and in vitro (6, 16). To investigate whether CD11b$^+$ macrophages in BALF would form lymphatic-like vessels, cells from BALF of IPF subjects and healthy volunteers were analyzed by flow cytometry to isolate a CD45$^+$/CD14$^+$/CD11b$^+$ population, which was grown in Matrigel (BD Biosciences) . No significant differences in the percentages of CD14$^+$/CD11b$^+$ cells in BALF were found between the 2 groups ($P = .542$) (Fig. S7).

When grown in Matrigel for 31 days, CD11b$^+$ alveolar macrophages from 2 of 4 subjects with IPF formed tube-like structures with diameters of ≈120 μm (Fig. 4*A*). Fluorescent staining of the cells with CellTracker Orange and Hoechst allowed visualization and imaging of the tubes deep within the matrix (Fig. 4*B*) and 3-dimensional reconstruction of the tubular structure (Fig. 4*C–F* and Movie S1). In contrast, CD45$^+$/CD14$^+$/

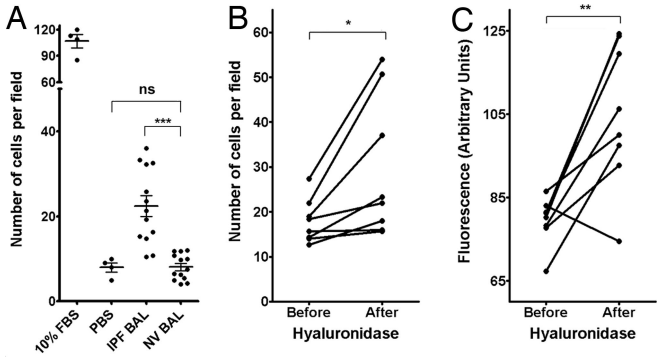

Fig. 3. Migration of lymphatic endothelial cells is induced by BALF from subjects with IPF in vitro and enhanced by treatment of BALF with hyaluronidase. (*A*) Cultured LECs were incubated in migration assays with BALF from subjects with IPF and from healthy volunteers. LEC migration was significantly greater in assays with the BALF from the subjects with IPF (***$P < .005$). FBS (10%) and PBS were used as positive and negative controls, respectively. IPF BALF was incubated at 37 °C overnight without or with hyaluronidase. This treatment generated small-fragment hyaluronic acid with increased LEC migration and proliferation activities. (*B*) Hyaluronidase treatment significantly increased the effects of IPF BALF on LEC migration (*$P < .05$). (*C*) Hyaluronidase treatment also increased the effect of IPF BALF on the proliferation of EGFP-expressing LECs (**$P < .01$).

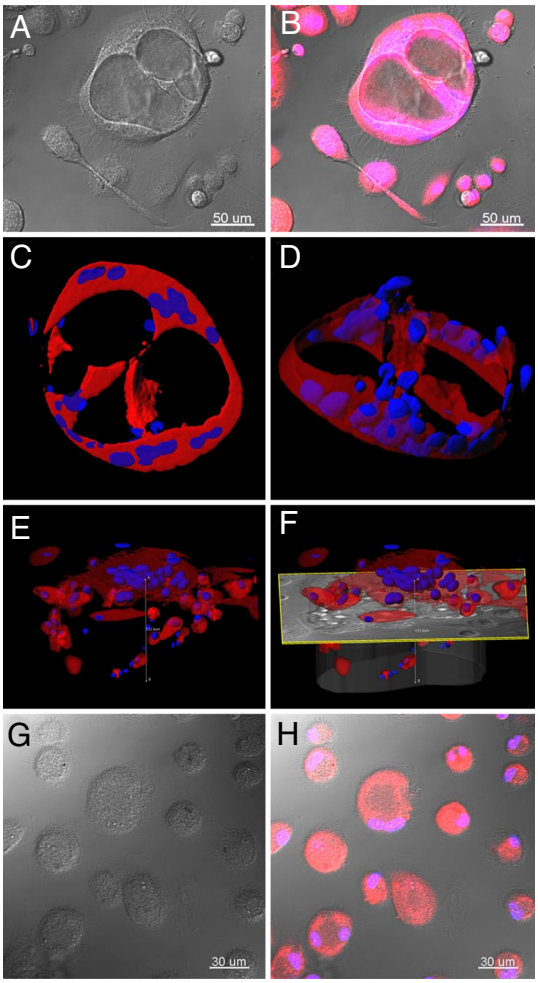

Fig. 4. CD11b$^+$ alveolar macrophages in IPF develop tube-like structures in vitro. CD11b$^+$ alveolar macrophages were cultured in Matrigel for up to 31 days and inspected under white light, or after fluorescent labeling of cytoplasm (CellTracker Orange) and nuclei (Hoechst). Large tube-like structures (150 μm diameter) were observed when cells from subjects with IPF were cultured. Representative tubular structures are shown in DIC (*A*) and fluorescence-overlaid images (*B*). Series of confocal images were collected along the *z*-axis up to depths of $\approx$120 μm and imported in Imaris software to reconstruct 3-dimensional renderings of these tubes (*C–F*). These images reveal large (100 μm deep), complex cellular structures with lumens consistent with vessel-like structures. In contrast, as shown in DIC (*G*) and overlaid fluorescence (*H*) images, CD11b$^+$ alveolar macrophages from healthy volunteers did not form tube-like structures.

CD11b$^+$ cells from 5 healthy volunteers did not form tubular structures when grown in Matrigel (Fig. 4*G* and *H*). CD45$^+$/CD11b$^-$ cells from subjects in both groups did not form tubular structures (data not shown).

We further investigated whether the tube-like structures formed by cultured CD11b$^+$ alveolar macrophages from subjects with IPF expressed lymphatic markers and found expression using anti-podoplanin and anti–LYVE-1 antibodies (Fig. 5*A–C*). Although the cells from healthy volunteers were reactive with anti–LYVE-1 antibodies, they did not form the tube-like structures after 31 days in culture.

Discussion

Here we report for the first time the presence of newly formed lymphatic vessels in IPF. Lymphatic vessels were found early in the disease process and increased in size with increasing disease severity. We have identified 2 potential mechanisms for this lymphangiogenic response. Specifically, our data demonstrate that short-fragment hyaluronic acid present in the BALF from subjects with IPF enhanced LEC migration and proliferation, and that CD11b$^+$ alveolar macrophages from subjects with IPF can transdifferentiate into LECs.

New lymphatic vessels associated with tissue injury and repair are thought to arise from existing lymphatic vessels (17). Normal lung parenchyma is generally devoid of lymphatics, except for lymphatic vessels within bronchovascular tissue. However, lymphatic vasculature was identified in alveolar spaces of IPF lung, suggesting a role for progenitor cells. Because bronchoalveolar fluid contains abundant macrophages, which can serve as progenitors for LECs (6), we explored the possibility that a subpopulation of alveolar macrophages may transdifferentiate into LECs. Consistent with this possibility, we found that CD11b$^+$ alveolar macrophages formed lymphatic-like tubes that expressed LYVE-1 and podoplanin when grown in a 3-dimensional matrix. Notably, transdifferentiation of CD11b$^+$ alveolar macrophages was observed in cells from subjects with IPF, but not in those from healthy volunteers. Although this capacity of CD11b$^+$ macrophages has been described in animal models (6, 18), our findings of transdifferentiation of macrophages from the lung in human disease are novel.

It is interesting that CD11b$^+$ alveolar macrophages isolated from healthy volunteers expressed LYVE-1, but did not form tubular structures. This finding seems to suggest that lymphangiogenic substances in the alveolar microenvironment in IPF may have long-standing effects, or perhaps may remain associated with CD11b$^+$ alveolar macrophages that promote transdifferentiation into LECs. Alternatively, it is possible that proteins capable of inhibiting lymphangiogenesis exist in the normal alveolar milieu and may induce partial long-term suppression of transdifferentiation of CD11b$^+$ alveolar macrophages into LECs. Although the mechanism of alveolar macrophage transdifferentiation in IPF is not fully understood, functional differences in alveolar macrophages derived from subjects with IPF and healthy volunteers have been reported previously (11, 19–21). Further investigation into the regulation of CD11b$^+$ alveolar macrophage transdifferentiation in normal and disease conditions may elucidate this process.

In inflammatory conditions, the growth of lymphatic vessels mirrors that of blood vessels (17, 22, 23). We investigated whether short-fragment hyaluronic acid, which can enhance the development of blood vasculature in IPF (24), is also capable of stimulating lymphangiogenesis. We found hyaluronic acid in the alveolar interstitium in the subjects with IPF. In the lung, hyaluronidase (which cleaves hyaluronic acid) can be produced by fibroblasts, epithelial cells, and alveolar macrophages, but the mechanism responsible for generating short-fragment hyaluronic acid in vivo is unknown (25). We found that BALF from subjects with IPF, known to be enriched in hyaluronic acid (26), induced more migration of LECs than BALF from healthy volunteers. This difference in LEC migration cannot be explained by dilution of the BALF, because some measured proteins were higher in the BALF from healthy volunteers. Consistent with previous findings (14), incubation of IPF BALF with hyaluronidase generated larger amounts of short-fragment hyaluronic acid, which we found significantly increased LEC migration and proliferation. Furthermore, supplementation of healthy volunteer BALF with short-fragment hyaluronic acid increased LEC migration. The actions of hyaluronic acid on endothelial cells have been reported to be mediated through CD44 for proliferation and through RHAMM for migration (27); these receptors are likely to be redundant, however (28). These findings demonstrate the importance of short-fragment hyaluronic acid in the lymphangiogenic response in IPF, and suggest a new role for hyaluronic acid in the pathogenesis of fibrotic lung disease.

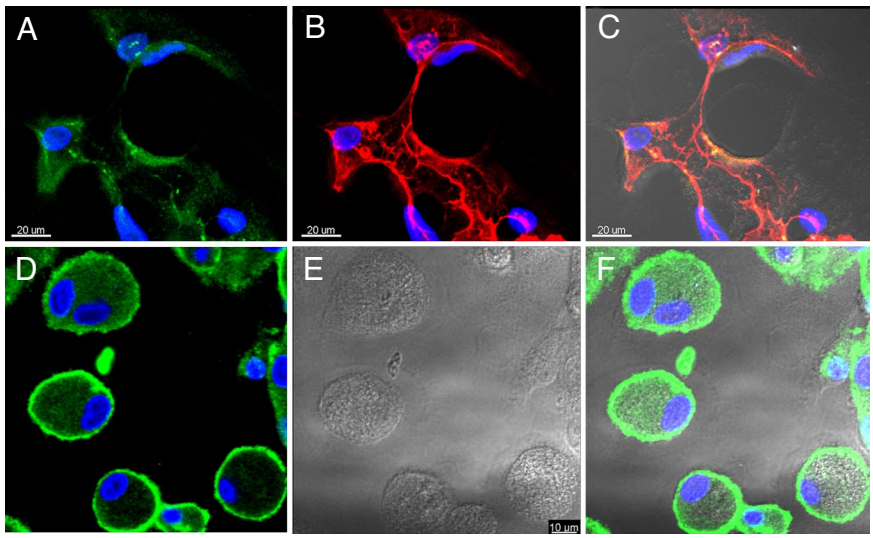

Fig. 5. Tube-like structures formed by CD11b$^+$ alveolar macrophages express LEC markers. After culturing in Matrigel for up to 31 days, cells were fixed, permeabilized, and stained by indirect immunofluorescence for LYVE-1 (green) (*A*) and podoplanin (red) (*B*). (*C*) A merged DIC and fluorescence image shows tube-like structures in the IPF samples that were reactive with LEC markers, anti–LYVE-1, and anti-podoplanin antibodies. (*D–F*) In contrast, cells from healthy volunteers show reactivity with anti–LYVE-1 antibodies outlining their periphery (*D*), without the formation of tube-like structures. Representative cells are shown in DIC and fluorescence-overlaid images. Cell nuclei were stained by DAPI (blue).

While investigating growth factors possibly involved in the lymphangiogenic process, we found that airway epithelium, alveolar epithelial cells, and alveolar macrophages all were immunopositive for VEGF-C in the lung sections of subjects with IPF (Fig. S8). The low levels of VEGF-C in the BALF samples may be explained by the destruction of alveolar spaces in IPF and resulting decreased production of VEGF-C by alveolar epithelial cells. Although total VEGF-C levels are lower, local production of VEGF-C may exist, which could be critical for lymphatic development. The low levels of VEGF-C, which is necessary for lymphatic vessel sprouting (29), may account for the increase in size, but not in number, of lymphatic vessels with increasing disease severity.

Lymphangiogenesis likely is detrimental in IPF, in which the lymphatic vessels appear early in the disease and in areas with relatively few other abnormalities. In a mouse model of asthma, the lymphangiogenic response, which followed the angiogenic response, failed to regress after the inciting stimulus was stopped (23). Moreover, in lymphedema, where the primary disturbance is in the lymphatic circulation, chronic injury results in skin fibrosis (30). The fibrotic process in IPF may be a result of chemokines, such as CCL21 secreted by LECs (31), which we found to be markedly elevated in the BALF of subjects with IPF. In IPF, CCL21 recruits immature dendritic cells to form organized lymphoid bodies (2). Intriguingly, recent evidence indicates that proliferation of IPF fibroblasts is enhanced by CCR-7, the receptor for CCL21 (32), suggesting that lymphatic endothelial cells could promote the fibrotic process in IPF.

As recognition of the importance of the lymphatic circulation in cancer and inflammation has increased, various inhibitors of lymphangiogenesis have been identified, some of which are currently in clinical trials for refractory cancer (33, 34). The potential use of lymphangiogenesis inhibitors in the treatment of IPF is complicated by 3 factors, however: (*i*) the known scientific concerns regarding the relevance of bleomycin-induced lung injury as a model for pulmonary fibrosis (35), (*ii*) the difficulty in evaluating the functionality of newly formed lymphatic vessels, and (*iii*) the mechanisms of action, because most lymphangiogenesis inhibitors interfere with VEGF-C and VEGF-D signaling by blocking ligand-binding or receptor action at the surface of LECs. Our data indicate that VEGF-C and VEGF-D probably are not the driving molecules of lymphangiogenesis in IPF. A better strategy would be to block the recruitment of dendritic cells and IPF-derived fibroblasts by LEC by blocking CCL21 or its receptor CCR-7 (36, 37).

Our findings provide strong evidence that lymphangiogenesis is a key element in lung injury and repair in IPF. Lymphangiogenesis is driven, at least partially, by mediators of inflammation (e.g., hyaluronic acid) and inflammatory cells (e.g., activated CD11b$^+$ macrophages). The roles of newly formed lymphatic vessels in the pathogenesis of disease remain to be elucidated, but defining the events leading to lymphatic vessel formation may offer new understanding and therapeutic options for this fatal disease.

Methods

Subject Selection. Subjects with IPF and healthy volunteers were enrolled in protocols approved by the Institutional Review Board of the National Heart, Lung and Blood Institute (99-H-0068 and 04-H-0211). The diagnosis of IPF was established according to previously published criteria (38, 39). Characteristics of subjects with IPF whose BALF was used in protein measurements, cell migration, and proliferation assays are summarized in Table S2. Subjects with IPF and healthy volunteers whose cells were studied in tubulation assays are described in Table S3. The healthy volunteers had no clinical evidence of lung disease and normal chest radiograph and pulmonary function test results.

Antibodies. The antibodies used in this study are listed in Table S4.

Immunohistochemistry and Immunofluorescence. Formalin-fixed, paraffin-embedded tissue sections obtained from lung explants or open lung biopsy from 12 subjects with IPF and 3 normal lungs, rejected for transplantation, were analyzed. To identify lymphatic vessels in tissue sections, monoclonal antibodies that are specific for podoplanin (D2–40), a marker of lymphatic endothelial cells (40), were used. To visualize blood vessel endothelial cells, anti-CD34 monoclonal antibody was used (41). CD34 is a panendothelial marker. Vessels reactive to anti-CD34 antibodies but not to anti–D2–40 antibodies were considered blood vessels. To identify hyaluronic acid, serial lung sections with or without pretreatment with *Streptomyces hyaluronictus* hyaluronidase (100 TRU; Seikagaku) at 60 °C for 2 h were incubated with 2 μg/mL of biotinylated hyaluronic acid–binding protein (bHABP; Seikagaku) overnight at 4 °C (42). Tissue sections also were incubated with anti–LYVE-1 rabbit polyclonal antibodies. Reactions were detected using TexasRed-labeled streptavidin (for bHABP) and FITC-labeled goat anti-rabbit antibodies (for LYVE-1). Nuclei were stained with DAPI.

Microscopy and Image Analysis. Tissue sections incubated with anti–D2–40 and anti-CD34 antibodies were inspected using wide-field microscopy with an

upright microscope (Nikon E-1000). Images were acquired with a Nikon DXM-1200CCD color digital camera using Nikon ACT1 software. Morphometric analyses were performed using 15 digital images per section imported into ImageJ v1.36b (National Institutes of Health) (43). The differentially immunostained lymphatic and blood vessels were identified and traced manually by a blinded investigator (B.A.W.); diameters, cross-sectional area, and perimeter were quantified.

Chemokine Levels. Chemokines were assayed using SearchLight proteome arrays (Pierce Biotechnology), as described in SI *Methods*.

Migration and Proliferation Assays. Cell chemotaxis and proliferation were assayed as described in SI *Methods*.

Fluorescence-Activated Cell Sorting. Bronchoscopy, BALF procurement and isolation of $CD45^+/CD14^+/CD11b^+$ are described in SI *Methods*.

Tubulogenesis Assay Using $CD11b^+$ Macrophages. FACS-sorted $CD45^+/CD14^+/CD11b^+$ cells were seeded at a density of 1.5×10^5 cells/mL in 500 μL of EBM-2 (Lonza) containing 3% FBS on a Matrigel layer prepared by mixing 100 μL of growth factor-reduced Matrigel with 100 μL of EBM-2 plated on coverglass 4-chamber slides (Nunc). Tube formation was monitored microscopically for 31 days (6). Cells in Matrigel were then stained with 2 μM CellTracker Orange (MP C 2927) and nuclei were stained with 10 μM Hoechst (33324) for 30 min at 37 °C. Cells were inspected with a Zeiss LSM510 confocal microscope using a 20 × 0.75NA objective and single optical sections. Series of images along the *z*-axis were collected at depths of up to ≈150 μm throughout the tube-like structures. The series of images were imported into Imaris 6.1.5 software (Bitplane), overlaid, and 3-dimensionally reconstructed. In addition, whole-mount preparations were analyzed by indirect immunofluorescence, using anti–LYVE-1 and anti-podoplanin antibodies as described previously. To assess cellular localization at higher resolution, images were obtained using a 40 × 1.4 NA plan Apochromat oil-immersion objective on a Zeiss 510 confocal microscope equipped with UV-Vis laser lines. Single optical sections and series of images along the *z*-axis were collected, overlaid, and analyzed.

Statistical Analysis. Data are expressed as mean ± SE for n number of samples. The significance of differences between means were evaluated using the paired or unpaired Student's *t*-test, the Mann-Whitney test, or ANOVA as appropriate. If a significant difference was found, then a group-by-group comparison was done. A P value $< .05$ was considered significant. Analyses were performed using GraphPad Prism version 4.00 for Windows.

ACKNOWLEDGMENTS. This study was supported by the Intramural Research Program of the National Heart, Lung, and Blood Institute (NHLBI), the National Human Genome Research Institute, and the National Cancer Institute. Partial support was provided by a Senior Fellowship from the Oak Ridge Institute for Science and Education (to Y.I.). We are indebted to Dr. Martha Vaughan for her valuable input and manuscript review. We also thank Drs. M. E. Monzon, S. M. Casalino-Matsuda, and R. M. Forteza (University of Miami Airway Biology Laboratory) and Dr. Zu-Xi Yu (NHLBI Pathology Core Facility) for constructive suggestions and recommendations. This research would not have been possible without the commitment of the patients of the Translational Medicine Branch and the staff of the National Institutes of Health Clinical Research Center.

1. Walter N, Collard HR, King TE Jr. (2006) Current perspectives on the treatment of idiopathic pulmonary fibrosis. *Proc Am Thorac Soc* 3:330–338.
2. Marchal-Somme J, *et al.* (2006) Cutting edge: Nonproliferating mature immune cells form a novel type of organized lymphoid structure in idiopathic pulmonary fibrosis. *J Immunol* 176:5735–5739.
3. Selman M, Pardo A (2006) Role of epithelial cells in idiopathic pulmonary fibrosis: From innocent targets to serial killers. *Proc Am Thorac Soc* 3:364–372.
4. Matsui K, *et al.* (2003) Lymphatic microvessels in the rat remnant kidney model of renal fibrosis: Aminopeptidase P and podoplanin are discriminatory markers for endothelial cells of blood and lymphatic vessels. *J Am Soc Nephrol* 14:1981–1989.
5. Teles-Grilo ML, *et al.* (2005) Differential expression of collagens type I and type IV in lymphangiogenesis during the angiogenic process associated with bleomycin-induced pulmonary fibrosis in rat. *Lymphology* 38:130–135.
6. Maruyama K, *et al.* (2005) Inflammation-induced lymphangiogenesis in the cornea arises from CD11b-positive macrophages. *J Clin Invest* 115:2363–2372.
7. Kajiya K, Detmar M (2006) An important role of lymphatic vessels in the control of UVB-induced edema formation and inflammation. *J Invest Dermatol* 126:919–921.
8. Kerjaschki D, *et al.* (2004) Lymphatic neoangiogenesis in human kidney transplants is associated with immunologically active lymphocytic infiltrates. *J Am Soc Nephrol* 15:603–612.
9. Kerjaschki D, *et al.* (2006) Lymphatic endothelial progenitor cells contribute to de novo lymphangiogenesis in human renal transplants. *Nat Med* 12:230–234.
10. Ristimaki A, *et al.* (1998) Proinflammatory cytokines regulate expression of the lymphatic endothelial mitogen vascular endothelial growth factor-C. *J Biol Chem* 273:8413–8418.
11. Jiang D, *et al.* (2005) Regulation of lung injury and repair by Toll-like receptors and hyaluronan. *Nat Med* 11:1173–1179.
12. Prevo R, *et al.* (2001) Mouse LYVE-1 is an endocytic receptor for hyaluronan in lymphatic endothelium. *J Biol Chem* 276:19420–19430.
13. Kamei M, *et al.* (2006) Endothelial tubes assemble from intracellular vacuoles in vivo. *Nature* 442:453–456.
14. Hamai A, Morikawa K, Horie K, Tokuyasu K (1989) Purification and characterization of hyaluronidase from *Streptococcus dysgalactiae*. *Agric Biol Chem* 53:2163–2168.
15. Stern R, Asari AA, Sugahara KN (2006) Hyaluronan fragments: An information-rich system. *Eur J Cell Biol* 85:699–715.
16. Schaberg T, Rau M, Stephan H, Lode H (1993) Increased number of alveolar macrophages expressing surface molecules of the CD11/CD18 family in sarcoidosis and idiopathic pulmonary fibrosis is related to the production of superoxide anions by these cells. *Am Rev Respir Dis* 147:1507–1513.
17. Karpanen T, Alitalo K (2008) Molecular biology and pathology of lymphangiogenesis. *Annu Rev Pathol* 3:367–397.
18. Maruyama K, *et al.* (2007) Decreased macrophage number and activation lead to reduced lymphatic vessel formation and contribute to impaired diabetic wound healing. *Am J Pathol* 170:1178–1191.
19. Ren P, *et al.* (2007) Impairment of alveolar macrophage transcription in idiopathic pulmonary fibrosis. *Am J Respir Crit Care Med* 175:1151–1157.
20. Savani RC, *et al.* (2000) A role for hyaluronan in macrophage accumulation and collagen deposition after bleomycin-induced lung injury. *Am J Respir Cell Mol Biol* 23:475–484.
21. Zhang-Hoover J, Sutton A, van Rooijen N, Stein-Streilein J (2000) A critical role for alveolar macrophages in elicitation of pulmonary immune fibrosis. *Immunology* 101:501–511.
22. Cursiefen C, *et al.* (2006) Time course of angiogenesis and lymphangiogenesis after brief corneal inflammation. *Cornea* 25:443–447.
23. Baluk P, *et al.* (2005) Pathogenesis of persistent lymphatic vessel hyperplasia in chronic airway inflammation. *J Clin Invest* 115:247–257.
24. Garantziotis S, *et al.* (2008) Serum inter-{alpha}-trypsin unhibitor and matrix hyaluronan promote angiogenesis in fibrotic lung injury. *Am J Respir Crit Care Med* 178:939–947.
25. Jiang D, Liang J, Noble PW (2007) Hyaluronan in tissue injury and repair. *Annu Rev Cell Dev Biol* 23:435–461.
26. Bjermer L, Lundgren R, Hallgren R (1989) Hyaluronan and type III procollagen peptide concentrations in bronchoalveolar lavage fluid in idiopathic pulmonary fibrosis. *Thorax* 44:126–131.
27. Savani RC, *et al.* (2001) Differential involvement of the hyaluronan (HA) receptors CD44 and receptor for HA-mediated motility in endothelial cell function and angiogenesis. *J Biol Chem* 276:36770–36778.
28. Nedvetzki S, *et al.* (2004) RHAMM, a receptor for hyaluronan-mediated motility, compensates for CD44 in inflamed CD44-knockout mice: A different interpretation of redundancy. *Proc Natl Acad Sci U S A* 101:18081–18086.
29. Karkkainen MJ, *et al.* (2004) Vascular endothelial growth factor C is required for sprouting of the first lymphatic vessels from embryonic veins. *Nat Immunol* 5:74–80.
30. Makinen T, *et al.* (2001) Inhibition of lymphangiogenesis with resulting lymphedema in transgenic mice expressing soluble VEGF receptor-3. *Nat Med* 7:199–205.
31. Bromley SK, Thomas SY, Luster AD (2005) Chemokine receptor CCR7 guides T cell exit from peripheral tissues and entry into afferent lymphatics. *Nat Immunol* 6:895–901.
32. Pierce EM, *et al.* (2007) Idiopathic pulmonary fibrosis fibroblasts migrate and proliferate to CC chemokine ligand 21. *Eur Respir J* 29:1082–1093.
33. Avraamides CJ, Garmy-Susini B, Varner JA (2008) Integrins in angiogenesis and lymphangiogenesis. *Nat Rev Cancer* 8:604–617.
34. Zwaans BM, Bielenberg DR (2007) Potential therapeutic strategies for lymphatic metastasis. *Microvasc Res* 74:145–158.
35. Gauldie J, Kolb M (2008) Animal models of pulmonary fibrosis: How far from effective reality? *Am J Physiol Lung Cell Mol Physiol* 294:L151.
36. Sasaki M, *et al.* (2003) Antagonist of secondary lymphoid tissue chemokine (CCR ligand 21) prevents the development of chronic graft-versus-host disease in mice. *J Immunol* 170:588–596.
37. Jensen KK, *et al.* (2003) Disruption of CCL21-induced chemotaxis in vitro and in vivo by M3, a chemokine-binding protein encoded by murine gammaherpesvirus 68. *J Virol* 77:624–630.
38. (2000) American Thoracic Society. Idiopathic pulmonary fibrosis: Diagnosis and treatment. International consensus statement, American Thoracic Society (ATS), and the European Respiratory Society (ERS). *Am J Respir Crit Care Med* 161:646–664.
39. (2002) American Thoracic Society/European Respiratory Society. International multidisciplinary consensus classification of the idiopathic interstitial pneumonias. *Am J Respir Crit Care Med* 165:277–304.
40. Van der Auwera I, *et al.* (2006) First international consensus on the methodology of lymphangiogenesis quantification in solid human tumours. *Br J Cancer* 95:1611–1625.
41. Miyata Y, *et al.* (2006) Lymphangiogenesis and angiogenesis in bladder cancer: Prognostic implications and regulation by vascular endothelial growth factors-A, -C, and -D. *Clin Cancer Res* 12:800–806.
42. Monzon ME, Casalino-Matsuda SM, Forteza RM (2006) Identification of glycosaminoglycans in human airway secretions. *Am J Respir Cell Mol Biol* 34:135–141.
43. Abramoff MD, Magelhaes PJ, Ram SJ (2004) Image processing with ImageJ. *Biophotonics Int* 11:36–42.